Telemanipulation with the DLR/HIT II Robot Hand Using a Dataglove and a Low Cost Force Feedback Device

Minas V. Liarokapis, Panagiotis K. Artemiadis and Kostas J. Kyriakopoulos

Abstract— **In this paper a series of teleoperation and manipulation tasks are performed with the five fingered robot hand DLR/HIT II. Two different everyday life objects are used for the manipulation tasks; a small ball and a rectangular object. The joint-to-joint mapping methodology is used to map human to robot hand motion, taking into account existing kinematic constraints such as synergistic characteristics and joint couplings. The Cyberglove II motion capture dataglove is used to measure human hand kinematics. A robot hand specific fast calibration procedure is used to map raw dataglove sensor values to human joint angles and subsequently through the mapping procedure, to DLR/HIT II joint angles. A novel low cost force feedback device is developed, in order for the user to be able to detect contact and perceive the forces exerted by the robot fingertips, during manipulation tasks. The design of the force feedback device is based on RGB LEDs that provide visual feedback and vibration motors that provide vibrotactile feedback.**

Index Terms: Telemanipulation, Teleoperation, Force Feedback Device, Mapping Human to Robot Motion.

I. INTRODUCTION

Over the last decades a lot of studies have focused on teleoperation and manipulation with robotic arm hand systems. A common research direction is to map human to robot motion so as the robotic artifact not only to move in free space but also to grasp or manipulate everyday life objects or actively interact with the environment.

For doing so user's kinematics have been captured, using various motion capture systems (e.g. vision based, flex sensors, IMUs etc.), while the forces exerted by the robotic artifacts have been measured with appropriate force sensors mounted e.g. at the fingertips of robot hands. Regarding hand motion mapping four major methodologies were proposed during the last years; the fingertip mapping, the joint-to-joint mapping, the functional pose mapping and the object

Minas V. Liarokapis and Kostas J. Kyriakopoulos are with the Control Systems Lab, School of Mechanical Engineering, National Technical University of Athens, 9 Heroon Polytechniou Str, Athens, 15780, Greece. Email: `mliaro | kkyria @mail.ntua.gr`

Panagiotis K. Artemiadis is with the ASU Human-Oriented Robotics and Control (HORC) Lab, School for Engineering of Matter, Transport and Energy, Ira A. Fulton Schools of Engineering, Arizona State University, 501 E. Tyler Mall, ECG 301, Tempe, AZ 85287-6106, USA. Email: `panagiotis.artemiadis@asu.edu`

specific mapping (using a virtual object). Fingertips mapping methodology was proposed in [1], [2], [3], [4] and [5] and is based on a forward/inverse kinematics mapping for each finger. More specifically, the forward kinematics of each human finger are computed and the positions of the human fingertips in 3D space are derived. Then the inverse kinematics for each robot finger are computed to conclude to the sets of angles that lead to the same human and robot fingertips positions in 3D space. The joint-to-joint mapping was used in [6] and later on in [7] and is a quite simple one-to-one joints angles mapping between the human and the robot hand. The simplicity of this method, has led many researchers to use it in order to map the human kinematics captured from a calibrated dataglove to various robot hands. It must be noted that in free space the postures replicated by the robot system are identical to the human master hand postures, as human and robot finger links have same orientations. Functional Pose Mapping [8] places both the human and the robot hands in a number of similar functional poses and a relationship between each human and robot joint is found, using for example the least squares fit method. Finally the object-specific mapping originally proposed in [9] assumes that a virtual sphere is held between the human thumb and index fingers. The parameters of the virtual object (size, position and orientation), are scaled independently and non-linearly to create a corresponding virtual object in the robot hand workspace. The virtual object, can be then used to compute the robot fingertip locations. The object-specific mapping was extended with very interesting results in [10] and [11], where human synergies were mapped to robot hands with dissimilar kinematics.

Various methods for teleoperation of multifingered robot hands using calibrated datagloves, have been proposed in the past. In [9] authors proposed an advanced calibration procedure where the thumb and index fingertips remain in contact approximating - due to rolling motion and soft tissue deformations - a closed kinematic chain. Moreover they mapped, using the object-based mapping approach, human index and thumb motion to a two fingered robot hand. In [5] cyberglove calibration is performed with a vision system, marking all human hand fingertips with coloured LEDs and using two stereo cameras to record the 3D position of thumb, index, middle and ring fingers. Force sensors were built into the HIT/DLR hand and the CyberGrasp (Cyberglove Systems) exo-skeleton was used to create one dimensional resistive force feedback per finger. In [12] the authors teleoperated the three fingered Barrett hand using a cyberglove (with position mapping), while the robot hand

was equipped with force sensors and the CyberGrasp system was once again used for force feedback. A recent study [13] proposes a task space framework for gesture based telemanipulation with a five fingered robot hand following the design principles of DLR/HIT II. The latter approach utilizes a library of task specific gesture commands, which replaces the conventional mapping between the human and the robot hands. Extensive experimental validation of the proposed method is performed using a series of manipulation tasks performed by the 15 DoFs robot hand. Finally in [14] a hybrid mapping combining some of the best features of the aforementioned mapping methodologies, is proposed. Approach is experimentally validated with teleoperation and manipulation tasks performed with the four fingered Schunk Anthropomorphic Hand (SAH).

Regarding force feedback the related literature focuses on different approaches ranging from vibro-tactile feedback, to visual and auditory. Most of the studies concern devices providing vibro-tactile feedback. In [15] the VibroTac, an ergonomic device using vibration motors to provide vibrotactile feedback is proposed, while in [16] a wearable vibrotactile feedback suit (for the whole arm hand system) based on vibrotactile actuators, is presented. Other studies focus on a mixture of sensory information including visual and vibrotactile feedback, like [17] where authors propose the RemoTouch, a system providing both tactile and visual feedback to the user. Finally in [18] different feedback strategies for shared control in telemanipulation studies are presented. More specifically authors compare different feedback methods and determine what combinations of force, visual and audio feedback provide the best performance.

In this paper we present a complete framework for teleoperation and manipulation with the five fingered robot hand DLR/HIT II. For doing so we captured human hand motion with the Cyberglove II motion capture dataglove, we performed a robot hand specific calibration of the dataglove values (that takes into account robot joint limits), we used the joint-to-joint human to robot motion mapping methodology and we developed a novel low-cost force feedback device based on RGB LEDs (Light-Emitting Diodes) and vibration motors. The RGB LEDs are first proposed in this study as an efficient low-cost alternative for providing force feedback. An extensive validation of the methods proposed in this study is performed using experimental paradigms involving teleoperation tasks, in unconstrained 3D space, as well as manipulation tasks with everyday life objects (a small ball and a rectangle). An accompanying video containing all the experiments conducted for system testing and for verification purposes, further validates our claims.

The rest of the document is organized as follows: Section II describes the apparatus used in this study, Section III focuses on the different methods proposed for the telemanipulation with a robot hand using a low cost force feedback device. The results and the experimental validation of the whole scheme are presented in Section IV while Section V concludes the paper and discusses the future directions.

II. APPARATUS

A. DLR/HIT II

The hand that we use in this study is the DLR/HIT II five fingered robot hand, which has a total of fifteen degrees of freedom (DoFs), three DoFs for each finger (two DoFs for finger flexion-extension and one DoF for finger abduction-adduction). The last two joints of each finger are coupled using a mechanical coupling based on steel wire (with a transmition ratio 1:1).

B. Cyberglove II Motion Capture System

In order to capture human hand motion, the Cyberglove II (Cyberglove Systems) motion capture dataglove was used. The Cyberglove II performs data collection at a frequency of 100Hz. Appropriate data acquisition software was written in C++ in order for the Cyberglove II to be used through the linux operating system that we use for the control of DLR/HIT II (Ubuntu 12.04 x86). Moreover a fast robot hand specific calibration procedure was also developed in C++ (official data acquisition and calibration software are available only for Windows OS).

C. A Low Cost Force Feedback Device based on RGB LEDs and Vibration Motors

In order for the user of the teleoperation scheme to be able to "perceive" the forces exerted by the robot fingertips (e.g. during object manipulation) we developed a low cost-force feedback device based on RGB LEDs and vibration motors. In this section we present the hardware specifications for the arduino open-source physical computing platform, the RGB LEDs and the vibration motors that were used to develop the device. Moreover we also present the different modules that formulate the aforementioned device: the RGB LEDs based module and the vibration motors based wrist band.

1) Arduino based Architecture: Arduino [19] is an open-source physical computing platform based on a simple I/O board and a development environment that implements the Processing/Wiring language. More specifically for the development of the force feedback device we used the Arduino Mega, a microcontroller board based on the ATmega2560 (high-performance, low-power micro-controller). Arduino Mega has 54 digital input/output pins (of which 14 can be used as PWM outputs), 16 analog inputs, 4 UARTs (hardware serial ports), a 16 MHz crystal oscillator, a USB connection, a power jack, an ICSP header, and a reset button. The Arduino Mega is compatible with most shields designed for the Arduino Duemilanove or Diecimila making future upgrades easy to implement. Arduino was used in our project as it has an insignificant cost and is widely available in the market. It must be noted that the main disadvantage of Arduino Mega is the fact that it has quite big dimensions, but any microcontroller platform could have been used for our purposes (e.g. possibly a smaller or even a lighter solution like arduino nano).

Arduino   RGB LED   Vibration Motor

Fig. 1. The arduino platform, a RGB LED and a vibration motor.

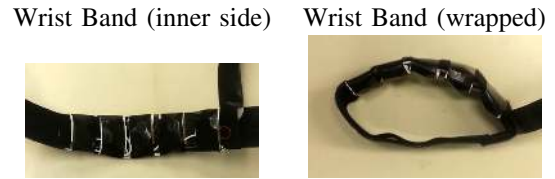Wrist Band (inner side)   Wrist Band (wrapped)

Fig. 3. Screenshot of the vibration motors based wrist band. One can notice that the vibration motors are enclosed in the inner side of the Velcro tape that we used to create the wrist band. Velcro tape was used, for the force feedback device to be low-cost and light-weight.

Flexiforce Sensor and Adapter   Phidgets Interface Kit 888

Fig. 4. Flexiforce sensor, Flexiforce adapter and Phidgets Interface Kit 888.

2) RGB LEDs and Vibration Motors: The RGB LEDs that we used are the RGB Piranha common cathode LEDs (Brightek Electronics co.) with the 5mm width. The RGB LEDs color ranges are the following; Red (400 - 700 mcd), Green (1000 - 1500 mcd) and Blue (400 - 500 mcd) and their dimensions; width: 0.76 cm, length: 0.76 cm and height: 1 cm. More details for the RGB LEDs can be found in [20].

The vibration motors that we used are 10 mm shaftless vibration motors (Precision Microdrives). The main advantages of the selected vibration motors are their low cost, low weight and small size. These three characteristics are very significant for the implementation of an affordable light-weight force feedback device. The vibration motors have the following characteristics: 3 V voltage, 10 mm frame diameter, 3.4 mm body length, 1.2 g weight, 2.5-3.8 V voltage range, 12000 rpm rated speed and 0.8 G vibration amplitude. More details regarding the vibration motors can be found in [21].

3) RGB LEDs based Wrist Band Module: The RGB LEDs based wrist band module consists of 5 RGB LEDs used to represent visually (fading from blue to red) the amount of force exerted from each robot finger. RGB LEDs relative positions have been chosen to be similar to the finger positions (following the order; thumb, index, middle, ring and pinky), in order for the optical feedback to be more easily interpreted by the user and associated with the corresponding finger.

Fig. 2. Screenshot of the RGB LEDs based module. RGB LEDs are positioned so as for their relative positions to be similar to those of the human fingers. The RGB LEDs from left to right correspond to the following fingers; thumb, index, middle, ring and pinky. Such a positioning helps the user to more easily associate the RGB LEDs with the corresponding fingers.

4) Vibration Motors based Wrist Band Module: The vibration motors based Wrist Band module consists of 5 vibration motors used to represent the amount of force exerted from each finger of the five-fingered robot hand through proportional skin vibrations. Vibration motor positions have been chosen so as to be uniformly distributed around the wrist in order to be as easy as possible for the user to interpret the provided vibrations.

5) Force Measuring Module: A force measuring module was developed, in order to capture the forces exerted by the robot fingertips. The module consists of: a Phidget Interface Kit 8/8/8 (I/O Board from Phidgets [22]), 5 flexiforce sensors (force sensors, one for each finger) and 5 flexiforce sensor adapters. Appropriate software written in C++ was used to perform data acquisition, using the force measuring module from the planner PC (Ubuntu 12.04 x86).

The force sensors used are FlexiForce sensors (Tekscan Inc.) which are ultra-thin and flexible printed circuits [23]. Some important characteristics of the FlexiForce sensors are; the paper-thin construction, the flexibility and their durability. FlexiForce force sensors can measure forces between almost any two surfaces and can be used to different environments. Moreover they have better force sensing properties, linearity, hysteresis, drift, and temperature sensitivity than other thin-film force sensors. Their "active sensing area" is a circle at the end of the sensor with diameter of 1 cm. In case that the specifications of the experiment require very low or very high forces exerted and if we want to measure these forces more precisely, the force measuring module can be used with different types of flexiforce sensors, providing ranges 0 - 10 lbs (0 - 4.4 N), 0 - 25 lbs (0 - 110 N) or even 0-100 lbs (0 - 440 N). Finally in order to interface the Tekscan FlexiForce sensors to the phidget interface, the five flexiforce adapters that appear in Fig. 4 were used.

III. METHODS

A. Kinematic Model of the Human Hand

The kinematic model of the human hand that we use consists of four kinematically identical fingers (index, middle, ring and pinky) with three rotational DoFs for flexion-extension and one rotational DoF for abduction-adduction. The thumb is modeled with two rotational DoFs for flexion-extension, one rotational DoF for abduction-adduction and
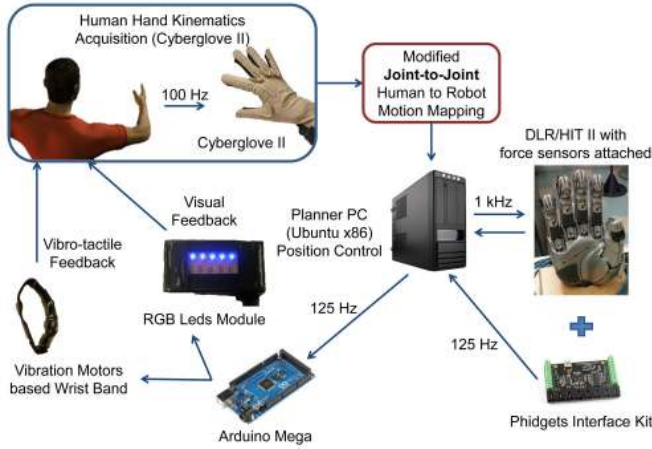
Fig. 5. Block diagram of the proposed scheme architecture.

one rotational DoF to model the palm mobility that allows the thumb to oppose to other fingers.

B. Robot Hand Specific Fast Cyberglove Calibration

In order to calibrate the Cyberglove II motion tracking system, we developed a new calibration module, based on:

- The aforementioned simplified kinematic model of the human hand that consists of 20 DoFs.
- Tuning of sensor gains (to estimate joint angles from raw sensor values), using two different postures and a free movement phase.

The two postures used during the advanced calibration procedure, appear in Fig. 6. The first posture is used to measure the raw cyberglove sensor values when all human flexion and abduction/adduction DoFs are in zero position in joint space. The second posture is used to measure the maximum possible cyberglove sensors raw values that correspond to the maximum abduction/adduction of all human hand fingers. It must be noted that these values differ among subjects, and are used in order to conclude to specific bounds of the values that the Cyberglove II may provide to the PC that performs position control of the DLR/HIT II.

Fig. 6. The two postures used by the calibration procedure. The zero values posture and the maximum abduction/adduction posture.

It's quite typical for the human hand to be more dexterous than a multifingered multi-DoF robot hand [24]. Moreover in most cases the human hand has greater joint limits than the robot hand. Thus if we perform a direct join-to-joint mapping

between the human and the robot hand we may lead the robot hand to exceed its limits (software/hardware) damaging some finger, or even causing inter-finger collisions.

The free movement phase used by the calibration procedure manages to measure the maximum values reported in terms of raw cyberglove sensors values, for each joint of the human hand. Thus in free movement users are instructed to "explore" the finger workspaces, in order to store also the maximum values for each finger (flexion/extension and abduction/adduction). In order to conclude to those gains that will linearly map the raw values of the Cyberglove II flex sensors, to the corresponding DLR/HIT II joints angles, we used the robot hand joint limits. To compute the gain for each DoF, we proceed as follows:

$$k_q = \frac{q_{max}}{|c_{max} - c_{zero}|} \tag{1}$$

where k_q is the gain for each DoF, q_{max} is the maximum value that a robot DoF can achieve (max joint limit) for the specific DoF, c_{max} is the maximum value of the Cyberglove II flex sensors that was measured and c_{zero} is the value of the Cyberglove II flex sensors, measured at the "zero" posture. It must be noted that the whole calibration procedure comes with a simple user interface and lasts less than 30 seconds. The gains computed are stored in automatically created files, for further use with the data collection software or the DLR/HIT II planner mechanisms.

C. Joint to Joint Mapping of Human to Robot Hand Motion

Regarding the DLR/HIT II robot hand, human to robot motion mapping is performed using a modified version of the well known joint-to-joint mapping methodology proposed in [6] and [7], based on the robot hand specific Cyberglove II calibration. As we have already mentioned the last two joints of each robot finger of the DLR/HIT II are coupled with a mechanical coupling based on a steel wire. Thus, we are not able to map both the measurements of the Distal Interphalangeal Joint (DIP) and the Proximal Interphalangeal Joint (PIP) of human hand, to the robot hand. In this study we choose to use the cyberglove values of the PIP joints of the human hand and map them to both the PIP and consequently (due to the coupling) to the DIP joints of the robot hand. The choice to use the PIP joint is supported by the fact, that human is able to flex PIP independently, but not DIP due to tendon coupling. Thus if we had selected the DIP there would be cases in which the user would flex only the PIP joint of the human hand and the corresponding robot finger wouldn't move as DIP value measured from the Cyberglove II would be zero. MetaCarpoPhalangeal (MCP) joints of the human hand are directly mapped using a one-to-one mapping to the MCP joints of the robot hand. Regarding abduction/adduction of robot fingers, for the middle finger, abduction and adduction movements are discarded and the DoF is kept fixed, as it cannot be measured by the Cyberglove II. All other abduction/adduction joint angles for the rest fingers are mapped one-to-one.

D. Mapping Exerted Forces to RGB LEDs Color Information and Vibration Amplitude

Regarding RGB LEDs, each led has three different color intensity values (one for each color) that can be controlled through the arduino platform. The value of each color can range from 0 (off state) to 255 (higher state) so in order to create the different color variations, we fuse different intensity levels of different colors. In this study we chose to represent the absence of force exertion with blue color and the maximum possible force exertion with red color. Thus we set a l_{blue} threshold (e.g. $l_{blue} = 50$, 20% of total range), for the blue color to illuminate the led when there is not force exertion and red color is $l_{red} = 0$. Then in order to map exerted forces to color alternations, we simply map them to proportional fusing values of the red color. The gain that linearly maps exerted forces to red color values is computed as follows:

$$k_{red} = \frac{256}{f_{max}} \qquad (2)$$

where f_{max} is the value of the flexiforce sensor for the maximum force exertion that is expected to happen and 256 is the range of red color values. l_{blue} and f_{max} can be set according to the specifications of each study, resulting to different force sensitivities for the whole system.

Regarding the vibration motors mapping, we simply used a proportional mapping using a gain k_{vibr} equal to the ratio defined with nominator the maximum voltage v_{max} that can be fed to the vibration motors and denominator the maximum selected force f_{max} that can be exerted by the robot fingertips. The gain for this proportional mapping is computed as follows:

$$k_{vibr} = \frac{v_{max}}{f_{max}} \qquad (3)$$

IV. RESULTS AND EXPERIMENTAL VALIDATION

In order to validate the efficiency of the proposed methods, a series of experimental paradigms were executed with the DLR/HIT II robot hand. Those paradigms included a free space exploration phase where the DLR/HIT II was teleoperated in different postures in unconstrained 3D space, while the motion imposed by the user was far from typical (different speeds and configurations were tested for all fingers). The second task was a combination of grasp, squeeze and rotation movements for a small plastic ball and a rectangle. In Fig. 7 we can see a series of screenshots presenting different postures executed during the first task, while in Fig. 8 a similar series of screenshots is used to depict the activity during the manipulation tasks execution. For a clearer understanding of the methods proposed in this paper as well as for a "first hand" evaluation of the robot hand "response" during the experiments, the reader should consult the accompanying video, which is available at the following url:

https://www.youtube.com/watch?v=MmK1QmLHajk

As we can see in the manipulation tasks appeared in the video, optical feedback is of outmost importance especially for those cases where occlusions occur between the user and the robot hand fingertips (e.g. caused by the objects grasped).

Fig. 7. Different postures of the human and robot hands, representing the different instances of the teleoperation tasks. The Cyberglove II motion capture system was used to teleoperate the DLR/HIT II robot hand in different postures, performing different motions with various speeds.
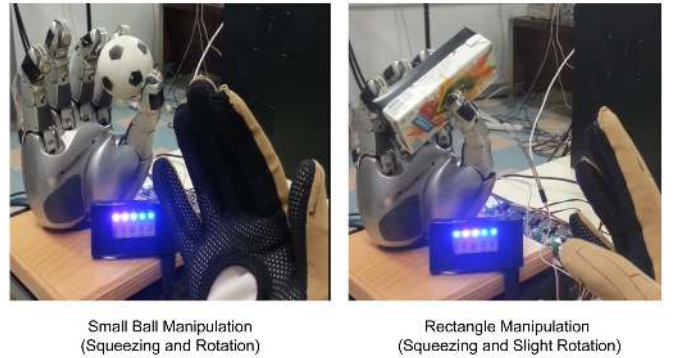

Fig. 8. Images depicting instances of the executed manipulation tasks, involving two everyday life objects: a small ball and a rectangle.

DLR/HIT II has a maximum tolerance of 10 N force that can be applied at the fingertips, thus the absence of a system that is able to detect contact as well as the amount of force exerted, may lead to severe damages of the robot fingers. It must be noted that in the screenshots appeared in Figures 7 and 8 when small amounts of forces are exerted, they mainly appear as changes of LEDs luminosities. Moreover the user is able to easily change the sensitivity of the color alternations changing the threshold of the blue color value during colors fusion (the RGB led module can be adjusted to be more sensitive, representing better lower force values). Finally, it's evident in the video that in some cases the fingers may contact the object with some part which is not covered with force sensors, thus in order to refine our study and improve the efficiency of our system we plan to integrate new force sensors, covering a greater part of the each finger.

V. Conclusions and Discussion

In this paper we presented a complete system for teleoperation and telemanipulation with the five fingered robot hand DLR/HIT II. A Cyberglove II was used to capture human hand kinematics and a modified version of the joint-to-joint mapping methodology was used to map human to robot hand motion. Moreover, a novel low-cost force feedback device based on RGB LEDs and vibration motors - that can provide real-time feedback of the forces exerted by a robot hand - was used so as for the user to be able to perceive the forces exerted by the robot fingertips. The choice to use both a visual and a vibro-tactile module to provide a mixture of sensory information for force feedback, was based on the hypothesis that can lead to more easily interpreted by the user results. The efficacy of the proposed methods is proved, using extensive experimental paradigms with the robot hand, performing different teleoperation and manipulation tasks. The accompanying video further validates our claims.

Regarding future directions the authors plan to conduct new experiments involving a wide set of manipulation tasks, as well as to extend the proposed scheme, in order to perform telemanipulation of everyday life objects with the Mitsubishi PA10 DLR/HIT II robot arm hand system. Such an application will experimentally validate the efficiency of the human to robot motion mapping scheme that we proposed in [25]. The final scheme will guarantee the execution of a specific functionality in task-space and then having accomplished such a prerequisite, will optimize anthropomorphism of structure or form, using some metric of Functional Anthropomorphism. A preliminary simulated paradigm of the whole arm hand system teleoperation, can be found in the video appearing at the following url:

```
https://www.youtube.com/watch?v=iKNIJTMlcCA
```

VI. Acknowledgements

References

[1] J. Hong and X. Tan, "Calibrating a vpl dataglove for teleoperating the utah/mit hand," in *Robotics and Automation, 1989. Proceedings., 1989 IEEE International Conference on*, may 1989, pp. 1752 –1757 vol.3.

[2] T. H. Speeter, "Transforming human hand motion for telemanipulation," *Presence: Teleoper. Virtual Environ.*, vol. 1, no. 1, pp. 63–79, January 1992.

[3] R. Rohling, "Optimized fingertip mapping and hand modeling for telemanipulation," Master's thesis, McGill University, 1993.

[4] M. Fischer, P. van der Smagt, and G. Hirzinger, "Learning techniques in a dataglove based telemanipulation system for the DLR hand," in *IEEE International Conference on Robotics and Automation (ICRA)*, 1998, pp. 1603–1608.

[5] H. Hu, X. Gao, J. Li, J. Wang, and H. Liu, "Calibrating human hand for teleoperating the HIT/DLR hand," in *IEEE International Conference on Robotics and Automation (ICRA)*, vol. 5, April 2004, pp. 4571–4576.

[6] M. Ciocarlie, C. Goldfeder, and P. Allen, "Dexterous grasping via eigengrasps: A low-dimensional approach to a high-complexity problem," in *Robotics: Science and Systems Manipulation Workshop - Sensing and Adapting to the Real World*, 2007.

[7] ——, "Dimensionality reduction for hand-independent dexterous robotic grasping," in *IEEE/RSJ International Conference on Intelligent Robots and Systems (IROS)*, November 2007, pp. 3270–3275.

[8] L. Pao and T. Speeter, "Transformation of human hand positions for robotic hand control," in *IEEE International Conference on Robotics and Automation (ICRA)*, vol. 3, May 1989, pp. 1758–1763.

[9] W. B. Griffin, R. P. Findley, M. L. Turner, and M. R. Cutkosky, "Calibration and mapping of a human hand for dexterous telemanipulation," in *ASME IMECE 2000 Symposium on Haptic Interfaces for Virtual Environments and Teleoperator Systems*, 2000.

[10] G. Gioioso, G. Salvietti, M. Malvezzi, and D. Prattichizzo, "An object-based approach to map human hand synergies onto robotic hands with dissimilar kinematics," in *Proceedings of Robotics: Science and Systems*, Sydney, Australia, July 2012.

[11] ——, "Mapping synergies from human to robotic hands with dissimilar kinematics: an object based approach," in *IEEE ICRA 2011 Workshop on Manipulation Under Uncertainty*, Shanghai, China, May 2011.

[12] A. Peer, S. Einenkel, and M. Buss, "Multi-fingered telemanipulation - mapping of a human hand to a three finger gripper," in *Robot and Human Interactive Communication, 2008. RO-MAN 2008. The 17th IEEE International Symposium on*, aug. 2008, pp. 465 –470.

[13] N. Lii, Z. Chen, M. Roa, A. Maier, B. Pleintinger, and C. Borst, "Toward a task space framework for gesture commanded telemanipulation," in *RO-MAN, 2012 IEEE*, sept. 2012, pp. 925 –932.

[14] L. Colasanto, R. Suarez, and J. Rosell, "Hybrid mapping for the assistance of teleoperated grasping tasks," *Systems, Man, and Cybernetics: Systems, IEEE Transactions on*, vol. 43, no. 2, pp. 390 –401, march 2013.

[15] S. Schatzle, T. Ende, T. Wusthoff, and C. Preusche, "Vibrotac: An ergonomic and versatile usable vibrotactile feedback device," in *RO-MAN, 2010 IEEE*, sept. 2010, pp. 670 –675.

[16] J. Lieberman and C. Breazeal, "Tikl: Development of a wearable vibrotactile feedback suit for improved human motor learning," *Robotics, IEEE Transactions on*, vol. 23, no. 5, pp. 919 –926, oct. 2007.

[17] D. Prattichizzo, F. Chinello, C. Pacchierotti, and K. Minamizawa, "Remotouch: A system for remote touch experience," in *RO-MAN, 2010 IEEE*, sept. 2010, pp. 676 –679.

[18] W. Griffin, W. Provancher, and M. Cutkosky, "Feedback strategies for shared control in dexterous telemanipulation," in *Intelligent Robots and Systems, 2003. (IROS 2003). Proceedings. 2003 IEEE/RSJ International Conference on*, vol. 3, oct. 2003, pp. 2791 – 2796 vol.3.

[19] Arduino, "Open-source electronics prototyping platform based on microcontroller," http://www.arduino.cc, Feb. 2013.

[20] B. Electronics, "RGB Leds piranha 5mm," http://www.sparkfun.com/datasheets/Components/LED/1P05S3UGB01DA301.pdf, Feb. 2013.

[21] P. Microdrives, "10mm shaftless vibration motors," http://www.sparkfun.com/datasheets/Robotics/310-101_datasheet.pdf, Feb. 2013.

[22] Phidgets, "Plug and play building blocks for low cost usb sensing and control," http://www.phidgets.com, Feb. 2013.

[23] Tekscan, "Flexiforce sensors," http://www.tekscan.com/flexible-force-sensors, Feb. 2013.

[24] M. V. Liarokapis, P. K. Artemiadis, and K. J. Kyriakopoulos, "Quantifying anthropomorphism of robot hands," in *IEEE International Conference on Robotics and Automation (ICRA)*, May 2013.

[25] ——, "Functional anthropomorphism for human to robot motion mapping," in *21st IEEE International Symposium on Robot and Human Interactive Communication (RO-MAN)*, Sept. 2012, pp. 31–36.